

Manuscript version: Author's Accepted Manuscript

The version presented in WRAP is the author's accepted manuscript and may differ from the published version or Version of Record.

Persistent WRAP URL:

<http://wrap.warwick.ac.uk/132845>

How to cite:

Please refer to published version for the most recent bibliographic citation information. If a published version is known of, the repository item page linked to above, will contain details on accessing it.

Copyright and reuse:

The Warwick Research Archive Portal (WRAP) makes this work by researchers of the University of Warwick available open access under the following conditions.

Copyright © and all moral rights to the version of the paper presented here belong to the individual author(s) and/or other copyright owners. To the extent reasonable and practicable the material made available in WRAP has been checked for eligibility before being made available.

Copies of full items can be used for personal research or study, educational, or not-for-profit purposes without prior permission or charge. Provided that the authors, title and full bibliographic details are credited, a hyperlink and/or URL is given for the original metadata page and the content is not changed in any way.

Publisher's statement:

Please refer to the repository item page, publisher's statement section, for further information.

For more information, please contact the WRAP Team at: wrap@warwick.ac.uk.

The interaction of polymer dispersed liquid crystal sensors with ultrasound

R.S. Edwards, J. Ward, L.Q. Zhou and O. Trushkevych¹

Department of Physics, University of Warwick, Coventry, CV4 7AL, UK^{a)}

Polymer dispersed liquid crystals (PDLCs) have been shown to be sensitive to ultrasound through the acousto-optic effect. The acousto-optic response of PDLC was studied over a broad frequency range (0.3–10 MHz). We demonstrate that the displacements required to produce acousto-optic clearing of PDLC films can be as low as a few nanometers, which is at least 10^3 times smaller than the PDLC droplet size, 10^5 times smaller than the PDLC layer thickness, and of the order of the molecular size of the liquid crystal constituents. This suggests that the acousto-optic effect in PDLC is due to microscopic effects of LC reorientation under torques or flows, rather than LC reorientation through macroscopic droplet deformation. The displacement required for clearing is related to the frequency of operation via an exponential decay. We attribute the observed frequency response to a freezing out of the rotational motion around the short axis of the liquid crystal. The reported frequency dependence and displacements required indicate that the effects and materials described here could be used for ultrasound visualisation in a non-destructive testing context.

Liquid crystals (LCs) are sensitive to ultrasound fields^{1–6}. In 1971 Mailer et al. studied the birefringence of an aligned LC layer using a 10 MHz ultrasound transducer². This acousto-optic effect has been used to develop acoustography for non-destructive testing (NDT), whereby a thick, aligned layer of LCs can be used to image ultrasound after it has passed through a sample in a water bath, identifying defects within the sample^{1,7}. Recently, ultrasound has been used to control orientation in a LC cell with periodic patterns observed in the optical behaviour^{3,4}, with a variable focus lens developed⁵.

A LC-based sensor which was flexible and could operate outside of a water bath and without polarisers would bring many benefits. For this, polymer-dispersed LCs (PDLCs) could be used^{8,9}. In such materials droplets of LCs are suspended in a polymer matrix, with the refractive index of the matrix chosen to match that of the LCs in their aligned state. In the unaligned state the film is scattering to light, whereas as the LCs in the droplets are aligned, the film becomes clear. Changes in alignment can therefore be seen visually without the requirement for polarisers¹⁰.

The acousto-optic effect in aligned LC films is fairly well understood, but the underlying mechanisms are still debated^{6,11–13}. The mechanism of interaction of ultrasound with PDLCs is less clear. Several researchers have reported that ultrasound will clear PDLC films, with clearing of the whole film due to leaky wavemodes from a surface acoustic wave reported in^{14,15}. We have recently shown visualisation of acoustic fields using PDLC films, demonstrated by the clearing of a film on top of an air-coupled ultrasound transducer, with the cleared regions matching the regions of largest amplitude vibration during resonance for frequencies below 1 MHz.¹⁶

In order to build a PDLC-based ultrasound sensor, it is essential to quantify the sensitivity and ensure that it is suitable for typical ultrasound displacements used in

fields such as NDT. Similar work has been performed for driving of the clearing using an electric field, studying the saturation voltage and threshold required for clearing¹⁷. A full understanding of clearing must consider the ultrasonic displacement, frequency range of operation, and the clearing efficiency over this range. Ultrasound frequencies from 10s of kHz to 10s of MHz are used for NDT, depending on the application. This paper studies the behaviour of a PDLC sensor on an air-coupled ultrasound transducer over a wide range of frequencies. It is tempting to use excitation voltage for the air-coupled transducer directly, however, there is not necessarily a linear correlation between excitation voltage and displacement for an ultrasound transducer, and the relationship varies depending on position on the transducer and the mode shape^{18,19}. Instead, displacement was measured using an interferometer, while clearing as a function of displacement was quantified through photography and image analysis.

A 25 mm diameter flexural ultrasound transducer was used, comprised of a piezoelectric element glued onto an aluminium cap²¹. These are designed to operate at low frequencies (fundamental resonance around 50 kHz), but will also resonate at higher frequencies for higher-order modes. The transducer was driven by a continuous sine wave using a function generator with a 25 W RF power amplifier. The excitation voltage was varied to change the displacement of the cap surface. Imaging of two low frequency modes (the 6:0 axi-symmetric mode close to 300 kHz, and the 11:0 axi-symmetric mode around 730 kHz) using both laser vibrometer and PDLC sensor was presented in reference¹⁶.

The transducer was coated with a thin layer of pink UV-curable varnish, to ensure good optical contrast when observing clearing. The PDLC films were produced using E7 and Norland adhesive NOA68, at a concentration of 75% LC, drop-cast onto the varnish layer and covered with a glass slide with spacers to form a 100 μm thick film. NOA68 is a UV curable adhesive and has been shown to produce a good sensor for ultrasound when used with a high concentration of E7^{14,16}. The LC droplet size distribution was analysed using polarised optical mi-

^{a)} Electronic mail: o.trushkevych@warwick.ac.uk

r.s.edwards@warwick.ac.uk;

scopy. For this, a 25 μm film was produced using the same preparation parameters as the 100 μm films; the thinner film was less scattering and allowed detailed microscopic images to be acquired for analysis.

The set-up of the transducer and PDLC is shown in the inset to figure 1. Impedance analysis showed that adding the varnish and PDLC layers on top of the transducer changed its resonant frequencies by 5%. Displacement measurements had to be done on the transducer without the PDLC and top cover, and this was later taken into account when locating resonant frequencies. Ultrasound signals were generated for transducer resonant frequencies between 300 kHz and 10 MHz, with driving voltages of between 50 mVpp and 250 mVpp pre-amplifier.

Prior to application of the PDLC layer the transducer was characterised. Figure 1 shows the displacement measured at the centre of the transducer using an Intelligent Optical Systems two-wave mixer interferometer, with a bandwidth of 250 MHz, for an excitation voltage of 100 mVpp. Note that measurement at just this position will not identify all modes, only those with significant displacement at the centre. Many resonances are shown by the peaks, with optimal generation at frequencies below 3 MHz. Above 3 MHz several small amplitude peaks are observed, corresponding to higher order modes.

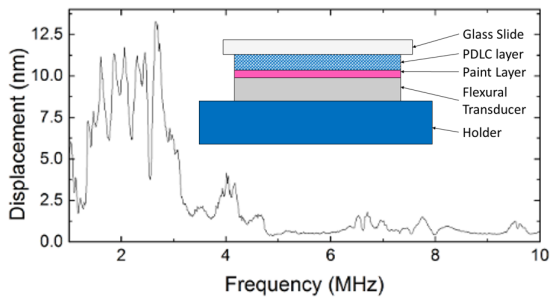


FIG. 1. Displacement of the air-coupled transducer for an excitation voltage of 100 mVpp, measured at the centre, omitting the fundamental frequency. The inset shows the set-up once the PDLC film has been applied.

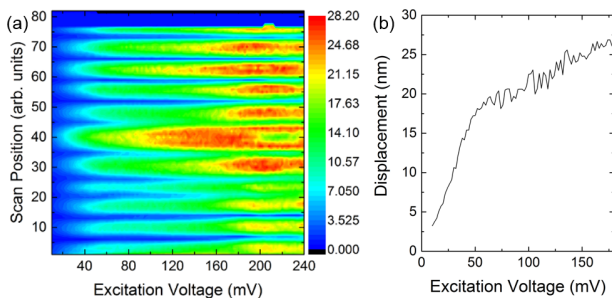


FIG. 2. (a) Colour plot of displacement during a scan across the centre of the transducer. (b) Displacement for the resonance. Both measured for the mode at 0.29 MHz.

Figure 2(a) shows the displacement measured during a one-dimensional (line) scan across the centre of the trans-

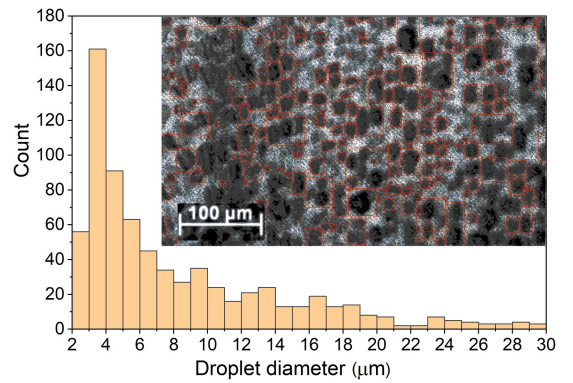


FIG. 3. PDLC structure for a 25 μm film, showing the calculated droplet diameter distribution; the inset shows droplet size analysis using Vision Builder AI from a polarised microscopy image.

ducer, plotted as a colour scale as a function of excitation voltage, at a frequency of 0.29 MHz. Note that the magnitude of the displacement at each point has been plotted, and hence the peaks and dips both show as maxima. At low excitation voltages the expected mode shape is observed. As the voltage is increased above 200 mV, the central peak shows a splitting, indicative of non-linear behaviour^{18,19}. Part (b) shows the displacement at the central point of the transducer plotted over the reduced excitation voltage range where linearity is observed in (a). The transducer shows two regions of behaviour, above and below 50 mV. All clearing measurements have therefore been done for voltages between 50 and 200 mVpp, and hence one linear region can be used for transducer calibration. Further characterisation of the transducer displacements was done for all modes studied using the PDLC sensor. All measurements were performed over the main linear region of the displacement vs. voltage curve.

The PDLC film structure was studied using polarised microscopy. The films were strongly polydisperse, and the droplets were not always spherical. It should be noted that film thickness acts as a low pass filter for droplet size, and extrapolating droplet size distribution in 100 μm film from studying a 25 μm thick film will not account for droplets with sizes above 25 μm . National Instruments software package Vision Builder AI & Visual Studio was used to analyse droplet size distributions on a micrograph with a $\times 10$ objective lens. This magnification gave good depth of field and allowed a large number of droplets to be visible at the same time. The inset to figure 3 shows that good recognition of droplets was achieved. However, some droplets were merged or slightly out of focus, giving an over- or under-estimation of droplet area in some cases. The largest number of droplets were under 4 μm in diameter, with a large population of droplets of 4-20 μm in diameter (Figure 3). The larger droplets dominate the occupied volume.

Photographs were taken at each voltage during clear-

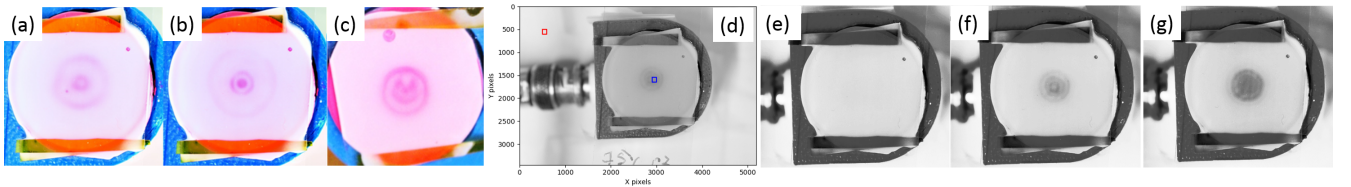


FIG. 4. Photographs taken of the modes at (a) 0.29 MHz, (b) 0.71 MHz, and (c) a happy mode at 6.65 MHz. (d) shows the regions chosen for ratio analysis of the 2.17 MHz mode, covering a region of clearing and a reference region. Driving voltages of (e) 50 mVpp (no clearing visible by eye), (f) 160 mVpp (clearing visible), (g) 200 mVpp (start of thermal clearing) for the 2.17 MHz mode. Note that image processing has been done to optimise for print only.

ing for different resonance modes using a DSLR camera (Canon EOS 600D). Care was taken to ensure that lighting conditions were identical for each photograph, with the aperture of $f/6.3$, shutter speed, and ISO of 800 kept constant. Before each sequence of photographs were taken the PDLC film was pre-warmed¹⁶, ensuring that the PDLC response time was sufficiently short to take photographs with a stabilisation time of only a few s. The time step between changing driving voltage and taking the photograph was kept constant. Figures 4(a)-(c) show several modes measured over a frequency range of 0.29–9.65 MHz, showing the broadband nature of the sensor; note that minor image processing has been applied for print quality. The low frequency resonances shown in (a) and (b) correspond to full vibrational motion of the aluminium cap. The smaller diameter displacement regions at the highest frequencies, such as that shown in (c), correspond primarily to vibration of the piezoelectric active element passing through the cap, as these are well above the standard operational frequency range for the cap.

Figures 4(e)-(g) show clearing of the mode at 2.17 MHz for several excitation voltages; note that again image processing has only been used to make these clear for printing. At low excitation voltages the mode clearing is not visible by eye. As the excitation voltage is increased the resonant mode shape becomes distinct, until by a driving voltage of 200 mVpp the energy input is enough to initiate thermal clearing.

Image analysis was used to quantify the changes in behaviour. To allow for any variation in lighting between different photographs in a sequence, photographs were turned into greyscale and analysis used the ratio between the greyscale value in a region where the PDLC film clears (blue box in figure 4(c)) to that of a reference region, taken away from the PDLC film (red box). The calculated ratio plotted against measured displacement is shown for several modes in figure 5(a). The data shows a very small initial rise, indicating that the PDLC film is becoming more scattering; this is not visible by eye and might be due to the onset of molecular reorientation in LC droplets. After this brief rise the ratio drops, indicating the onset of clearing, before it is visible by eye. Beyond a particular driving voltage the ratio levels off, indicating that the PDLC is saturated (fully cleared). All measurements were done while the mode shape was clear,

keeping away from the thermal clearing regime.

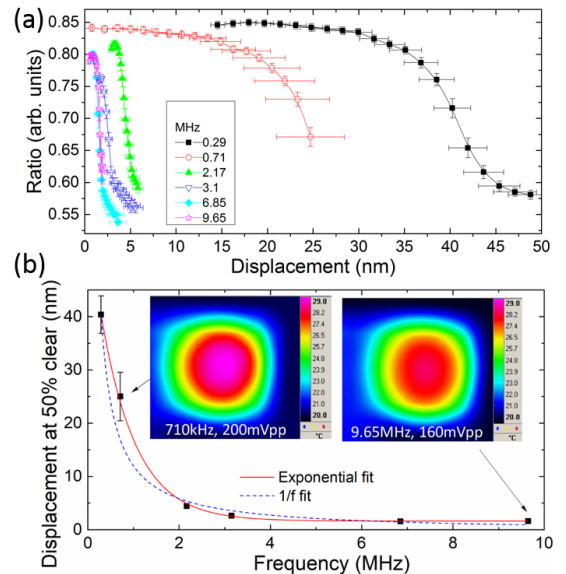


FIG. 5. (a) Ratios calculated from the photographs, showing clearing, as a function of displacement. (b) Displacement at 50% clearing. The insets show thermal images taken at two of the frequencies at 50% clearing.

Heating of piezoelectric transducers occurs and increases with excitation power and frequency²⁰. Raised temperatures increase the sensitivity of PDLC films to ultrasound¹⁶. The temperature of the transducer surface was monitored using a Cedex Titanium 20 thermal camera. A transducer with a paint layer was covered with black tape with known emissivity. The transducer was excited with voltages that are sufficient to obtain the acousto-optic effect at the reported frequencies. The temperature rise was very similar for all resonant modes studied, with heating to around 28°C for all modes (shown as the insets to figure 5(b)), enabling direct comparison of results from different frequencies. The observed clearing is not due to a thermal transition into the isotropic phase because it is observed when the transducer surface temperature is 30°C below the transition into the isotropic phase. Once the ultrasound is switched off, the heat takes around 60 s to dissipate, while the clearing pattern disappears within less than a second.

Displacements as small as a few nm are sufficient to clear the PDLC above a frequency of 1 MHz. This result is of great interest from both the physics and applications points of view. For applications, such displacements are within the range used in NDT. In terms of the physics, this can shed light onto the nature of the acousto-optic effect in PDLC. There are two possibilities for the nature: a macroscopic change in LC droplet shape that leads to LC reorientation within the droplet, or microscopic flows or torques that lead to molecular realignment. The magnitude of the displacements necessary to achieve acousto-optic clearing reported here seems to rule out any macroscopic processes. Assuming displacement of 5 nm, a film thickness of 100 μm and an average droplet diameter of 5 μm , the deformation of each droplet would be around 0.25 nm, a change of only $5 \times 10^{-3}\%$. For comparison, the individual rod-shaped molecules comprising E7 are around 1-2 nm in length. This suggests that a microscopic process is significantly more likely.

A clear dependence on frequency is observed, with lower frequencies requiring much higher displacements to clear. The curves were normalised using an S-curve fit to rescale them to cover a range from 1 (not cleared) to 0 (cleared), and the displacement which gave 50% clearing was found. This is plotted in figure 5(b). Two fits were performed; the $1/f$ fit would indicate a sensitivity to velocity, but a better fit is obtained from an exponential decay fit. The displacement required for 50% clearing drops to e^{-1} at around 0.75 MHz.

There are two main factors that may affect the frequency response of PDLC and LC: excitation wavelength vs LC droplet size, and relaxation behaviour of the LC. Where the excitation wavelength is much larger or much smaller than the LC droplet size, no frequency dependence is expected. For the case where the wavelength is similar to the droplet size, resonant effects may come into play. Depending on what mechanisms are responsible for the acousto-optic effect, two wavelengths are of interest: the wavelength of ultrasound in the film, and the viscous wavelength⁶. The acoustic wavelength of the ultrasound inside the PDLC is calculated based on the reported speed of sound in nematics^{22,23}, giving $\lambda_a \approx 2$ mm at 0.75 MHz. This is much larger than the PDLC droplet size (and even the PDLC film thickness), which rules out any resonant effects relating to direct interaction with the acoustic wave. The viscous wave has been postulated to be generated through acoustic excitation in aligned LCs layers at a rigid boundary (glass cell wall)⁶. It is not clear whether the concept is applicable to PDLC, as the geometry is different (droplets, boundaries with soft polymer). For LC layers, the viscous wavelength is calculated using⁶

$$\lambda_v = 2\pi \sqrt{\frac{2\eta_d}{\rho\omega}}, \quad (1)$$

where η_d is dynamic viscosity, ρ is density, and ω is frequency. The viscous wavelength in E7 is $\lambda_v = 25$ μm at 0.75 MHz, and 7 μm at 10 MHz. For the studied frequency range there are droplets with a size of the order

of the viscous wavelength, and hence resonant effects can not be fully ruled out. It should be noted that the polydispersity of the PDLC film in this study is very large and may complicate or mask any resonant behaviour, and the viscous wave concept may not be applicable to PDLCs. A focused study is needed to answer questions relating to the mechanisms of the acousto-optic effect in PDLC.

The observed frequency dependence may be associated with a relaxation process. For the acousto-optic effect in aligned LC²⁴, the dynamic response suggests two relaxation mechanisms - a slow one attributed to non-uniform flows in a standing wave field, and (a more pronounced) fast one attributed to a Fredericksz-type reorientation process. Both mechanisms are molecular level and are likely to be present in the studied PDLC. At low frequencies, there are many degrees of freedom for molecular motion (rotation etc), and many pathways for the input energy to be dissipated before it can realign the LC. Exciting the LC or PDLC above their relaxation frequencies will therefore result in less energy necessary to realign the LC, and therefore the sensitivity to excitation is expected to be higher.

A dielectric relaxation associated with freezing out rotation along the short molecular axis in E7²⁵ and in a E7-PMMA PDLC²⁶ has been reported for dielectric measurements at frequencies just above 1 MHz (note that the polymer and PDLC preparation process in reference²⁶ is different to that used here). Viciosa et al. report that increasing temperature and adding a polymeric substrate shifts the relaxation frequency up²⁵, so a dielectric relaxation in E7 as a PDLC at 28°C is expected to be above 1 MHz.

The acoustic frequency at which the displacement needed to change the optical properties of LC in PDLC drops by e is 0.75 MHz, obtained from the exponential fit to the data in figure 5(b). This may not be at the same frequency at which the LC's dielectric properties change, as probed by dielectric spectroscopy, even if the underlying relaxation process is the same. While the observed relaxation value is lower than expected compared to these other measurements, it is of the same order of magnitude. We believe that in the current study, the observed frequency dependence can be explained by relaxation in E7. Resonant effects cannot be completely ruled out, but are less likely.

In summary, the displacements required for acousto-optic clearing of PDLC films (75% wt of LC, glass cover on top) are between around 2 and 50 nm, depending on the frequency of excitation. Such small displacements are around 0.005% of the film thickness and 0.05%–0.5% of the droplet size, and are comparable to the molecular size of the constituents of the E7 LC mixture. Based on this value of displacement, we suggest that the observed acousto-optic effect in PDLC is a molecular-based process rather than a macroscopic change in droplet shape. The frequency dependence can be attributed to being primarily due to a relaxation of E7 associated with freezing out molecular rotation around the short axis. However,

resonant effects related to droplet size cannot be completely ruled out. A detailed study on a monodisperse PDLC film or a similar model system is necessary to answer this question.

The displacements and ultrasonic intensities required for acousto-optic clearing of PDLC above 1 MHz are comparable to those used during NDT. Further optimisation of the PDLC materials used would enable higher sensitivity. There is therefore significant promise for applying PDLC as a film sensor for detecting ultrasound in an NDT context.

This work was funded by the Research Centre in Non-Destructive Evaluation (RCNDE), the University of Warwick Materials Global Research Priority (GRP), and supported by Merck KGaA who provided LC materials. The IOS system was provided by ERC grant 202735. J. Ward was funded through the University of Warwick Undergraduate Research Scholarship Scheme.

- ¹JS Sandhu, RA Schmidt and PJ La Riviere, *Medical Physics* 36(6) 2324–2327 (2009)
- ²H Mailer, KL Likins, TR Taylor, and JL Ferguson, *Appl. Phys. Lett.* 18, 105 (1971)
- ³S Taniguchi, D Koyama, Y Shimizu, A Emoto, K Nakamura and M Matsukawa, *Appl. Phys. Lett.* 108, 101103 (2016)
- ⁴Y Shimizu, D Koyama, S Taniguchi, A Emoto, K Nakamura and M Matsukawa, *Appl. Phys. Lett.* 111, 231101 (2017)
- ⁵Y Shimizu, D Koyama, M Fukui, A Emoto, K Nakamura and M Matsukawa, *Appl. Phys. Lett.* 112, 161104 (2018)
- ⁶OA Kapustina, *Acoustical Physics* 54(2) 180–196 (2008)
- ⁷JS Sandhu, RW Schoonover, JI Weber, J Tawiah, V Kunin and MA Anastasio, *Advances in Acoustics and Vibration* 275858 (2012)
- ⁸JW Doane, NA Vaz, BG Wu and S Zumer, *Appl. Phys. Lett.* 48(4) (1986)
- ⁹D Coates, *J. Mater. Chem.* 5 2063–2072 (1995)
- ¹⁰D Cupelli, FP Nicoletta, S Manfredi, M Vivacqua, P Formoso, G DeFilpo and G Chidichimo, *Solar Energy Materials & Solar Cells* 93 2008-2012 (2009)
- ¹¹OA Kapustina, *Crystallography Reports* 59(5) 635–649 (2014)
- ¹²JV Selinger, MS Spector, VA Greanya, BT Weslowski, DK Shenoy and R Shashidhar, *Phys. Rev. E* 66 051708 (2002)
- ¹³AP Malanoski, VA Greanya, BT Weslowski, MS Spector, JV Selinger and R Shashidhar, *Phys. Rev. E* 69 021705 (2004)
- ¹⁴YJ Liu, X Ding, S Lin, J Shi, I-K Chiang and TJ Huang, *Advanced Materials* 23(14) 1656–1659 (2011)
- ¹⁵YJ Liu, M Lu, X Ding, ESP Leong, S Lin, J Shi, JH Teng, L Want, TJ Bunning and TJ Huang, *Journal of Laboratory Automation* 18 291–295 (2013)
- ¹⁶O Trushkevych, TJR Eriksson, SN Ramadas, SM Dixon and RS Edwards, *Appl. Phys. Lett.* 107(5) 054102 (2015)
- ¹⁷J Liu, X Liu and Z Zhen, *Materials Letters* 163 142–145 (2016)
- ¹⁸LQ Zhou, GB Colston, M Pearce, RG Prince, M Myronov, DR Leadley, O Trushkevych and RS Edwards, *Appl. Phys. Lett.* 111 (1) 011904 (2017)
- ¹⁹A Feeney, L Kang, G Rowlands, LQ Zhou and SM Dixon, *IEEE Sensors Journal*, 19(15) 6056-6066 (2019)
- ²⁰P Ronkanen, P Kallio, M Vilkkko and HN Koivo, *Micro-Nanomechanics and Human Science, and The Fourth Symposium Micro-Nanomechanics for Information-Based Society, Nagoya, Japan, 313-318* (2004)
- ²¹TJR Eriksson, SN Ramadas and S Dixon, *Ultrasonics*, 65 242-248 (2016)
- ²²AV Glushchenko, V Spermach and O Yaroshchuk, *International Journal of Fluid Mechanics Research* 30(3) 299-306 (2003)
- ²³ME Mullen, B. Luthi and MJ Stephen, *Phys. Rev. Lett.* 28(13) 799 (1972)
- ²⁴VA Greanya, AP Malanoski, BT Weslowski, MS. Spector and JV Selinger, *Liq. Cryst.*, 32(7), 933-941 (2005)
- ²⁵Viciosa MT, Nunes AM, Fernandes A, Almeida PL, Godinho MH and Dionisio MD, *Liquid Crystals* 29(3) 429-441 (2002)
- ²⁶ZZ Zhong DE Schuele WL Gordon, KJ Adamic and RB Akins, *Polymer Physics* 30(13) 1443-1449 (1992)